Transactions of the Materials Research Society of Japan 31[4] 845-852 (2006)

Preparation of Preform for Porous Ceramic-Matrix-Composite by the Pyrolysis of Phenolic Resin

Muhammad Akhtar Sharif [1], Yuzo Nakamura [2] and Hidekazu Sueyoshi [3]
1) Graduate school student, Graduate School of Science and Engineering
2) Department of Mechanical Engineering
3) Department of Nano-structured and Advanced Materials
Graduate School of Science and Engineering
Kagoshima University, Kagoshima, 890-0065, Japan

The aim of the present study is to fabricate preforms in order to obtain porous ceramic-matrix-composites (CMCs) with unique properties arising from porous structure. For this purpose, phenolic resin was mixed with Si powders and ZrO_2 nano-particles and then pyrolyzed at 1123 K. Pyrolysis of dry mixing of starting materials prior to the wet mixing led to the agglomeration of ZrO_2 particles and the formation of pores ranging from 10 μm to several 100 μm in diameter, resulting in the flexural strength of about 14 MPa. On the other hand, wet mixing with ethanol resulted in the formation of preforms with pores ranging from 0.8 μm to 10 μm in diameter and the uniform distribution of ZrO_2 particles in the matrix. The maximum flexural strength of preforms obtained by wet mixing was 56 MPa. XRD and XPS analyses suggested the formation of β-SiC in the composites. In addition, XRD analyses showed that the matrices of both preforms were amorphous carbon and XPS peaks of C, O, Si, Zr are broadened, suggesting the formation of many compounds during pyrolysis.

Keywords: Porous Ceramic-Matrix Composite, Pyrolysis; Microstructure, Flexural strength

1. INTRODUCTION

Porous ceramics have been recognized as very attractive materials for their functions originating from the properties of pores [1]. They are expected to be used for the catalysis, separation of gases and liquids [2-6], lightweight structural materials [5], biomaterials [5, 7, 8] and so on. However, the strength of porous ceramics is considerably low compared to dense ceramics, and one of the most significant developments required to porous ceramics is to improve their mechanical properties.

One of the methods to strengthen porous ceramics is to fabricate strongly bonded matrix like SiC between pores. In addition, the introduction of small pores into the matrix is favored because fracture strength of brittle materials decreases with increasing flaw size [6, 9, 10]. Another effective method for strengthening porous ceramics is to reinforce the matrix by incorporating second particles or fibers into the matrix [11, 12]. In order to attain these strengthening effects simultaneously during the synthesis of porous ceramics, it is necessary to prepare preforms of ceramic-matrix-composites (CMCs) with matrix in which fine pores and second particles are uniformly distributed.

It is well known that the pyrolysis of polymeric materials is a useful route to provide inorganic carbon matrix [13, 14]. Polymeric materials can be fluidized and decomposed during the heat treatment of pyrolysis. The decomposition of polymeric materials is associated with the generation of a variety of gases, which in turn make pores into the obtained matrix. The addition of silicon into carbon leads to the formation of SiC when the heating temperature is above 1673 K [15]. Further, it is expected that the porous SiC matrix may be toughened by incorporating hard particles into the matrix.

Zirconia is a well known material which has superior properties such as high mechanical strength, chemical durability, alkali resistance, heat resistance against oxidation and refractoriness [16]. The importance of zirconia in various technical applications makes the compound an interesting subject for research work. Over the past years, there has been an increasing interest in nanostructured ceramics for their lower sintering temperature and improved mechanical properties [17].

From the points of view mentioned above, phenolic resin was mixed with Si powders and ZrO_2 particles, and then heated at 1123 K in a closed copper tube in order to obtain the preform of SiC / ZrO_2 composites with a high density of fine pores.

2. EXPERIMENTAL PROCEDURES

2.1 Starting materials

The average grain diameters and weight fractions of solid phenolic resin (PR-50590B, SUMITOMO BAKELITE Co., Ltd. Japan), Si (FURUUCHI CHEMICAL Co., Ltd. Japan) and ZrO_2 (TOSOH-ZIRCONIA TZ-0, TOSOH Co., Ltd. Japan) powders used for the preparation of specimens are listed in Table I. In order to achieve 1 : 1 atomic ratio between carbon and silicon atoms in the matrix, the calculated ratio between phenol resin and silicon is 1 : 1.5. But considering the loss of carbon atoms due to evaporation and the formation of gaseous molecules (such as carbon dioxide and hydrocarbons) during pyrolysis, the designed weight of phenol resin involved in the mixture of the TZ-0 and Si powders is larger than the calculated value, as given in Table I.

Table I
Average grain size and mass fractions of the components in mixture.

Component	ZrO_2	Si	Phenol resin
Average grain size (μm)	0.40	1	35
Weight fraction (%)	25	25	50

2.2 Sample Preparation

2.2.1. Dry mixing

In preliminary we obtained a good microstructure by dry mixing. The powders of phenol resin, ZrO_2 and Si were mixed in a grinding bowl for 180 min. at room temperature. The weight fractions of these powders are listed in Table I. The mixture of powders was put into a copper tube of 100 mm length, 10 mm diameter and 1 mm thickness, and both ends of the tube were closed mechanically. Pyrolysis was carried out by heating the Cu tube in a furnace under a pressure of 15 mPa. The heating and cooling program is given below:
RT → 473 K (3.33 K/min), 60 min holding → 1123 K (3.61 K/min), 180 min holding→723 K (3.33 K/min) → RT (cooling in vacuum).

2.2.2. Wet mixing

In wet mixing, powders of ZrO_2 and Si (weight fractions of these powders are listed in Table I) were mixed in a grinding bowl for 180 min. at room temperature. In order to obtain slurry and homogeneous mixture, phenol resin was dissolved in 28 ml of ethanol at room temperature, and then added into the mixture of ZrO_2 and Si powders to make slurry. The slurry was poured into a copper tube and then pyrolyzed with the same heating and cooling program as explained in the dry mixing. The evaporation of ethanol and the decomposition accompanied by condensation reaction of the phenol resin took place during first holding at 473 K, while the specimens were pyrolyzed during second holding at 1123 K.

2.3. Properties and morphology investigation

Since the pyrolyzed specimens exhibited shrinkage, their weight loss and apparent density were measured. The microstructure of the polished specimens was observed using scanning electron microscopy (SEM; XL-30 ESEM Series, FEI Co. Ltd., Japan) and the energy dispersive spectrometer (EDS), equipped to the SEM, was used for the elemental analyses. The crystalline structure was observed by x-ray diffraction (XRD-6000S SHIMADZU Co. Ltd., Japan), which was performed with Cu irradiation (1.54060A°) at a scanning rate of 2 °/min in 2θ range between 20° and 80°. Chemical states of the atoms in the pyrolyzed composite were investigated by x-ray photoelectron spectroscopy (XPS; ESCA-1000, SHIMADZU Co. Ltd., Japan). Flexural strengths of the specimens were measured at room temperature using a three-point-bend-testing apparatus (span: 30 mm, cross head speed: 0.5 mm/min), which was mounted on a tensile testing machine (AG-1, 50kN, SHIMADZU Co. Ltd., Japan).

3. RESULTS AND DISCUSSION

3.1. Weight loss and apparent density

The weight loss and apparent density of dry mixed specimens pyrolyzed at 1123 K were examined. The average weight loss in the specimens was 19.70% (max.: 20.17%, min.: 19.03%), which is attributed to the degasification of molecules formed during pyrolysis. The average apparent density of specimens was 1.08 g/cm^3 (max.: 1.13 g/cm^3, min.: 1.01 g/cm^3). This lightweight composite is devoted to the formation of many pores.

The average weight loss in the wet mixed specimens was 31.64% (max.: 32.71%, min.: 30.75%). This larger value of weight loss is due to the evaporation of ethanol and molecules formed during pyrolysis. The average apparent density of the wet mixed composites was 1.85 g/cm^3 (max.: 1.96 g/cm^3, min.: 1.71 g/cm^3), which is about 18% smaller than that of graphite (density = 2.25 g/cm^3).

3.2. Morphological properties

3.2.1. Dry mixed specimens

Morphology of the dry mixed fabricated preform for porous CMC was observed with SEM. Figures 1(a) and 1(b) show the cross-sectional SEM photographs of the composites containing pores, small and large particles. The matrix is composed of uniformly distributed spherical pores with diameter ranging from several 10 μm to several 100 μm (Fig. 1(a)), small greyish particles ranging in diameter from several μm to several 10 μm (Fig. 1(b)) and large particles of several 10 μm in diameter with outer layer of thickness about 10 μm.

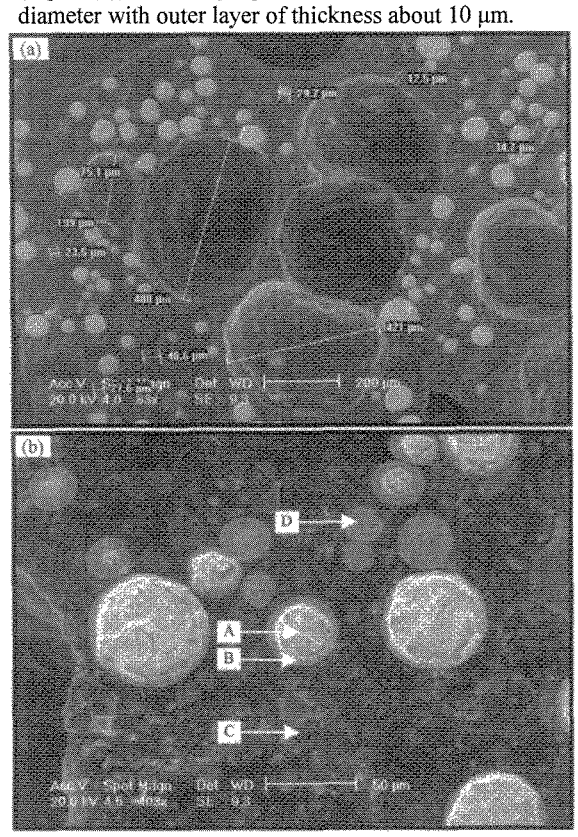

Fig. 1. SEM micrographs of cross-section of the dry mixed pyrolyzed preform; (a) matrix having large size pores and embedded particles, and (b) magnified view of small and large particles in the matrix.

In order to obtain the information of materials, EDS analyses were carried out at point A, B, C and D (Fig. 1(b)). The energy-dispersion profile of emitted x-rays

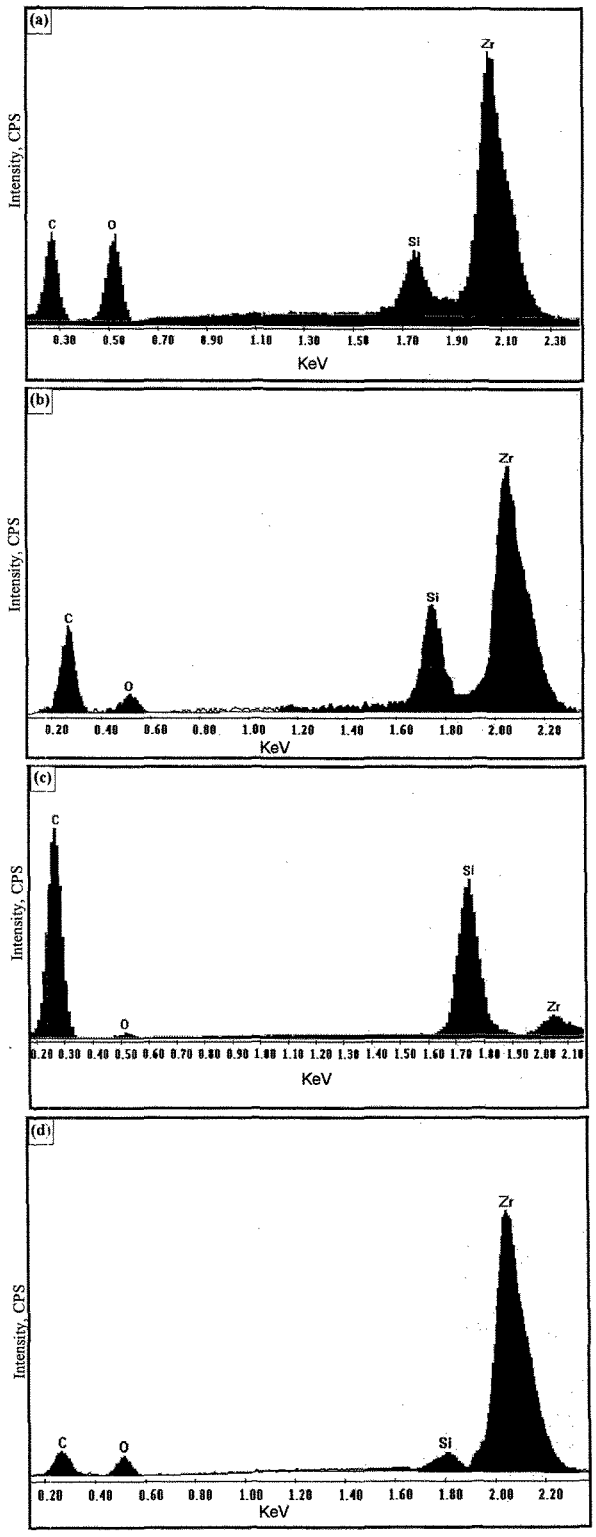

Fig. 2. EDS analyses of the dry mixed pyrolyzed preform; (a) point analysis of elements in the interior of large particle (point A of Fig. 1(b)), (b) point analysis of elements in the outer layer of large particle (point B in Fig. 1(b)), (c) point analysis of elements in the matrix (point C of Fig. 1(b)), and (d) point analysis of elements in the small particle (point D of Fig. 1(b)).

showed that in the interior of the large particle (Point A in Fig. 1(b)), Zr has highest peak than C, O and Si peaks as shown in Fig. 2(a). This fact shows that the interior of the particles is composed of Zr as a major element with C, O and Si. Fig. 2(b) shows that peak height of Si increases and that of O decreases in the outer layer of the large particle (Point B of Fig. 1(b)), also the peak height of Zr slightly decreases. In comparison to interior of the large particle, the outer layer is also composed of Zr as a major element with more Si and less O elements, while C almost remained constant. In the matrix (Point C of Fig. 1(b)), the peak of C is higher than the peaks of O, Si and Zr (Fig. 2(c)), which shows the existence of C in a larger amount in the matrix than other elements. The elemental analysis of greyish small particle (Point D of Fig. 1(b)) showed that the peak heights of C, O and Si are almost equal with highest peak of Zr, as shown in Fig. 2(d). Therefore, small particles are composed of Zr as a major element with small amounts C, O and Si elements. The peak heights C, O and Si elements in Fig. 2(a) were also nearly the same with highest peak of Zr. Thus, the EDS analyses suggested that the agglomeration of small particles was nucleated by the nano sized zirconia particles in powder mixing; and then these small particles were grown to large particles with larger amounts of C and Si elements in the outer layer.In addition, some reactions took place during the formation of small greyish and large bilayered particles (with inner white and outer greyish layer).

3.2.2. Wet mixed specimens

The cross-sectional SEM photographs of the wet mixed fabricated preform are shown in Figs. 3(a) and 3(b).

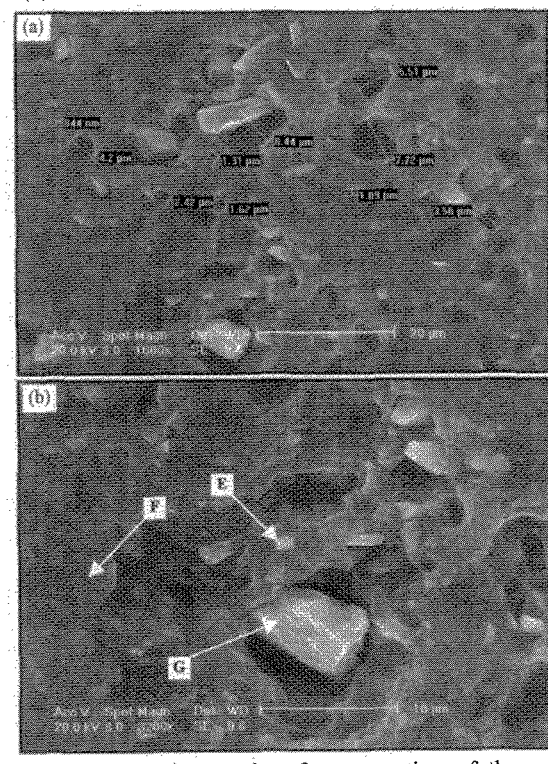

Fig. 3. SEM micrographs of cross-section of the wet mixed pyrolyzed preform; (a) matrix having micro pores and particles, and (b) enlarged cross-sectional view of particles in pores and matrix.

The matrix is composed of uniformly distributed micro pores of size ranging from 844 nm to 8.44 μm in diameter (Fig. 3(a)). A certain fraction of the pores were filled with particles (Fig. 3(b)). According to the SEM observations, the decrease in pore size and their filling with particles resulted in more apparent density of the wet mixed composite than that of the specimens made by dry mixing.

In order to obtain the information of materials, EDS analyses were carried out at point E, F and G (Fig. 3(b)) and are shown in Figures 4(a), 4(b) and 4(c), respectively. At point E (Fig. 3(b)), where a small white embedded particle exists in the matrix, Si showed the highest peak than the peaks of C, O and Zr (Fig. 4(a)).

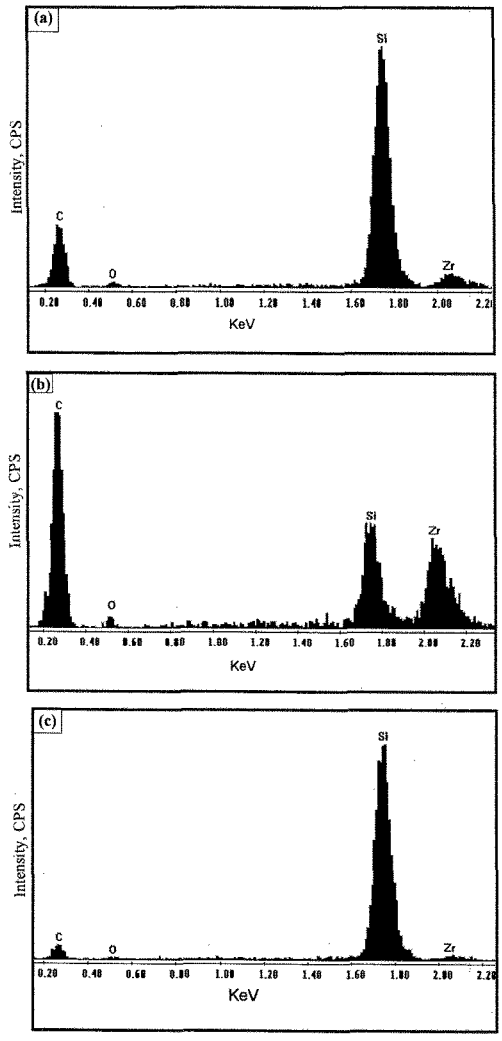

Fig. 4. EDS analyses of the wet mixed perform; (a) point analysis of elements in matrix particle (point E of Fig. 3(b)), (b) point analysis of elements in the matrix (point F in Fig. 3(b)), and (c) point analysis of elements in pore particle (point G of Fig. 3(b)).

This result suggests that the white particle is a Si-rich particle containing C, O and Zr. Carbon showed the highest peak (At point F in Fig. 3(b)) in the matrix than Si, O and Zr, as shown in Fig. 4(b). The low Si and Zr peaks indicate that Si and ZrO_2 particles are embedded in the C-rich matrix. The EDS analysis of large white particle in the pore (point G in Fig. 3(b)) revealed that white particles in the pores are composed of Si with small traces of C, O and Zr (Fig. 4(c)). The EDS point analyses of wet mixed pyrolyzed composite showed that matrix is composed of C as a major element; and Si-rich particles are embedded in matrix and pores. Since the average size of ZrO_2 particles is 400 nm, it is difficult to observe their distribution in the matrix. However, we can say that the agglomeration of ZrO_2 particles in the matrix does not take place in the present processing.

3.3. Structural analysis of the specimens by x-ray diffraction (XRD)

X-ray diffraction spectra obtained from dry mixed and wet mixed pyrolyzed preforms showed the similar behavior as shown in Figs. 5(a) and 5(b), respectively.

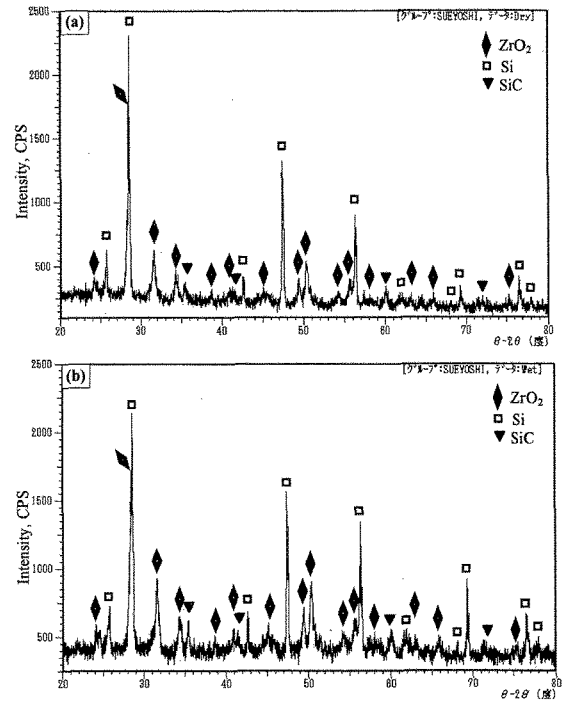

Fig. 5. X-ray diffraction spectra obtained from pyrolyzed performs; (a) dry mixed, and (b) wet mixed pyrolyzed preform.

The peaks at $2\theta = 28.4°$, 47.3°, 56.1° belong to (111), (220) and (311) planes of cubic crystalline silicon [19]. ZrO_2 has monoclinic form with peaks (-111), (111), (200) and (002) at $2\theta = 28.1°$, 31.4°, 34.1° and 35.3° respectively. Other peaks of Si and ZrO_2 are also indexed in Fig. 5(a) and 5(b). X-ray diffraction peaks around $2\theta = 35.6°$, 41.4°, 60.0° and 71.8° are (111), (200), (220) and (311) belong to cubic form silicon carbide (β-SiC), respectively [20, 21]. The peaks of carbon were not observed in XRD profile, which means that amorphous carbon exists in the pyrolyzed specimens.

3.4 X-ray photoelectron spectra investigations

X-ray photoelectron spectroscopy is a unique and unparalleled instrumental technique for obtaining detailed atomic elemental information and only non-destructive spectroscopic technique that can also yield data on molecular structures [22]. Thus, the observed XPS spectra of Si, C, Zr and O are mentioned below.

(Received August 1, 2006;Accepted August 10, 2007)

3.4.1. Silicon

XPS spectrum of Si $2p^{3/2}$ electrons obtained from the dry mixed pyrolyzed preform is shown in Fig. 6. The highest peak at 99.03 eV corresponds to Si, which is in agreement with the result of XRD analyses. The spectrum is broadened towards higher energies indicates that Si atoms are bound with other atoms. The peak at 99.95 eV corresponds to SiC, whose existence in cubic form was also observed in XRD analyses. It is reasonable to consider that XPS spectrum for Si $2p^{3/2}$ has a range with nearly the same intensity from 101.50 eV to 103.50 eV where chemical state of Si varies continuously from mono-oxide to fully-oxidized state of dioxide. Remarkable peaks are attributed to oxide layers of Si such as SiO and SiO2. Peak at the highest binding energy of 103.53 eV belongs to SiO_2 in the dry mixed pyrolyzed composites. The formed SiO and SiO_2 may be amorphous because XRD pattern of the composite did not reveal their crystalline existence. The peak at 101.52 eV corresponds to the deposited thin layer (about 300 nm) of silicon monoxide (SiO, 101.70 - 102.70 eV) [23].

Fig.7 shows XPS spectrum for Si $2p^{3/2}$ electrons obtained from the wet mixed pyrolyzed specimen. The peaks observed in the XPS spectrum indicate that chemical reactions occurred during the pyrolysis, because the electrons are emitted from a very thin surface layer of several 10 nm due to x-ray irradiation. Precise deconvolution of Si peaks led to the suggestion that SiO_2, SiO and SiC were formed in the pyrolyzed composite at a binding energy of 103.80 eV, 102.40 eV and 99.80 eV, respectively. The existence of SiC was also observed in XRD analyses and XPS spectrum for Si $2p^{3/2}$ electrons obtained from the wet mixed pyrolyzed specimen.

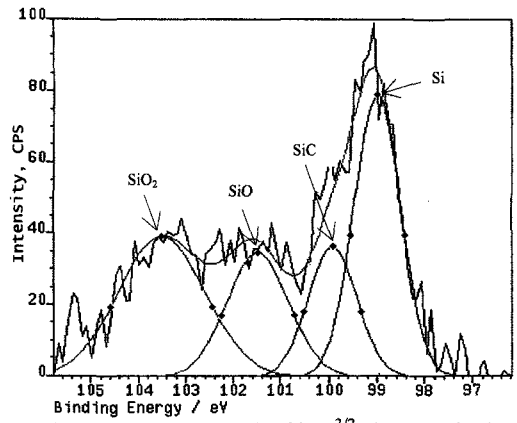

Fig. 6. XPS spectrum for Si $2p^{3/2}$ electrons in the dry mixed pyrolyzed specimen.

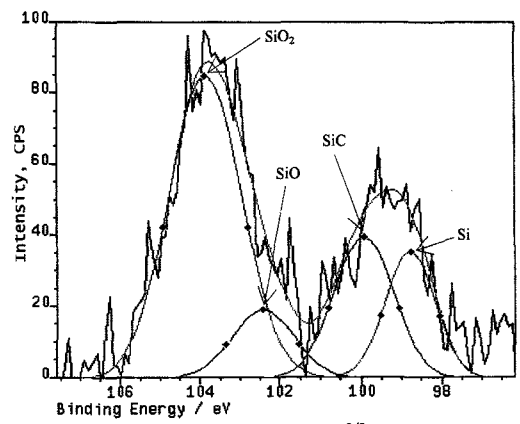

Fig. 7. XPS spectrum for Si $2p^{3/2}$ electrons in the wet mixed pyrolyzed specimen.

3.4.2. Carbon

XPS spectra of C 1s electrons obtained from the dry and wet mixed pyrolyzed preforms showed almost the similar behavior as shown in Fig. 8 and Fig. 9. The XPS spectra are broadened towards high-energy side and have several peaks. The highest peak at 284.06 eV originated from carbon present in the pyrolyzed composites. The other peaks are divided into lower and higher ones than 284.06 eV. The lower peak at 283.40 eV is considered to be attributed to C 1s in SiC. The formation of SiC was also observed in XRD analyses of the composites and XPS spectra for Si 2p electrons. The other higher energy peaks between 285.08 - 285.42 eV are assigned to hydroxyl (>C-OH) [24], peak at 286.30 eV is assigned to hydrocarbon in which carbon is bound to oxygen (C-O), between 287.34 - 288.49 eV to carbonyl (>C=O) and 290.13 - 290.92 eV to carboxylic (-COOH) functional groups [24]. The peaks lying between 288.50 - 289.50 eV corresponds to alkyl carbonate group (-O-CO-O-) [23]. These results suggest that formation of various organic compounds with different functional groups took place during the pyrolysis of phenol resin and these gaseous molecules were deposited on the inner surfaces of the closed pores.

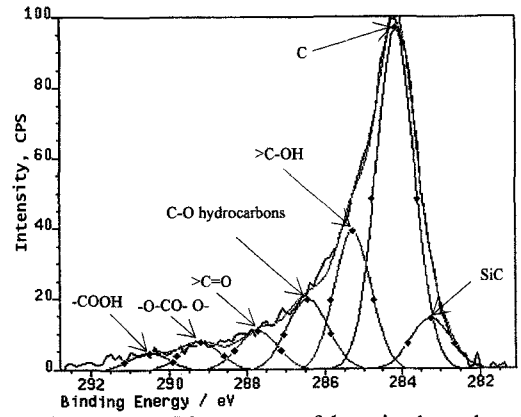

Fig. 8. C 1s XPS spectrum of dry mixed pyrolyzed phenol resin / ZrO_2 / Si composite.

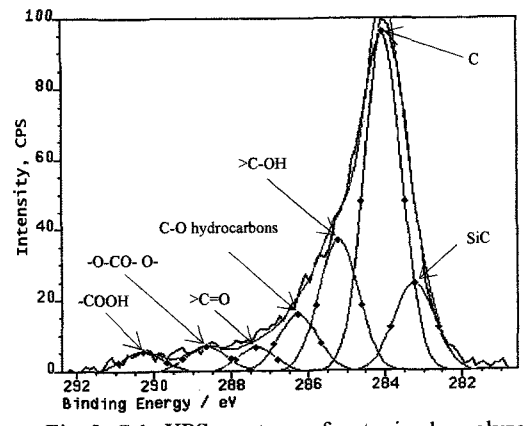

Fig. 9. C 1s XPS spectrum of wet mixed pyrolyzed phenol resin / ZrO_2 / Si composite.

3.4.3. Zirconium

XPS spectra of zirconium 3d electrons obtained from dry and wet mixed pyrolyzed preforms are shown in Fig. 10 and Fig. 11, respectively. In dry mixed pyrolyzed

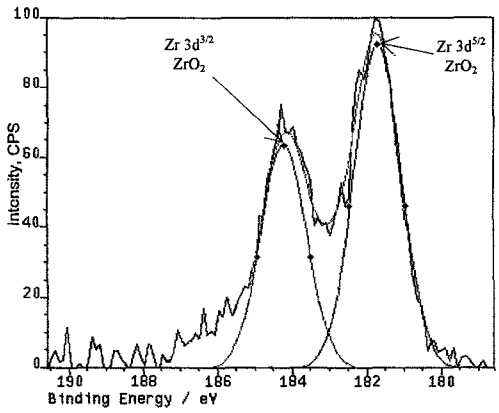

Fig. 10. XPS spectrum of Zr 3d electrons obtained from dry mixed pyrolyzed composite

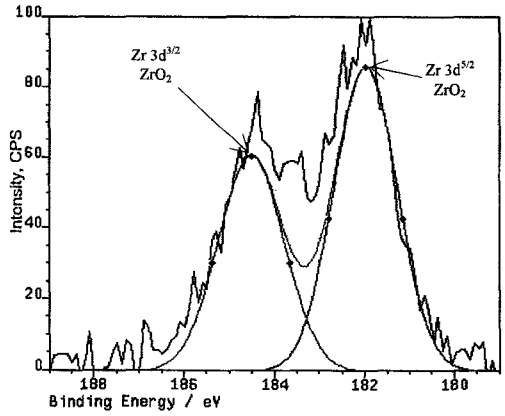

Fig. 11. XPS spectrum of Zr 3d electrons obtained from wet mixed pyrolyzed composite

phenol resin / ZrO_2 / Si composite, zirconium is involved in ZrO_2 for its $3d^{5/2}$ and $3d^{3/2}$ electrons at 181.73 eV and 184.25 eV, respectively, while in wet mixed pyrolyzed preform, zirconium is involved in ZrO_2 for its $3d^{5/2}$ and $3d^{3/2}$ electrons at 181.99 eV and 184.53 eV, respectively. However, in the present study, the binding energies of Zr $3d^{5/2}$ electrons involved in ZrO_2 obtained from dry and wet mixed pyrolyzed composites are slightly smaller than those reported by M. J. Guittet *et al* [25].

3.4.4. Oxygen

The XPS spectra of O 1s electrons obtained from dry and wet pyrolyzed preforms are shown in Fig. 12 and Fig. 13 respectively. The XPS spectra obtained from preforms revealed the presence of five peaks corresponding to ZrO_2 (529.90 - 530.70 eV), carbonyl (>C=O) or hydroxyl (>C-OH) group between 531.70 - 532.20 eV, SiO (532.50 eV), SiO_2 / C-O / -COOH between 533 - 534 eV and alkyl carbonate (-O-CO-O-) group (535.11 eV). XPS spectra for Zr 3d and Si 2p electrons also showed the existence of oxygen involved in ZrO_2, SiO_2 and SiO.

The formation of organic compounds containing carbonyl and alkyl carbonate functional groups was also revealed by XPS spectra of C 1s electrons. These gaseous compounds were produced during pyrolysis of phenol resin and caused the formation of pores. Those gaseous compounds which trapped in closed pores were deposited on the inner surfaces of pores.

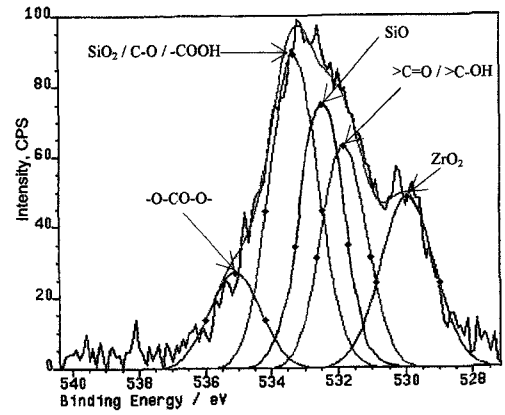

Fig. 12. XPS spectrum of O 1s electrons obtained from dry mixed composite.

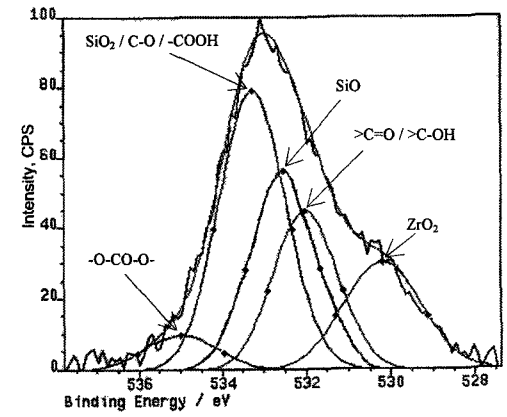

Fig. 13. XPS spectrum of O 1s electrons obtained from wet mixed composite.

S. Ishihara *et al.* suggested that the carbothermic reduction of SiO_2 may leads to the formation of SiC at 2073 K, as given in following reactions [26]:

$$SiO_2 + 3C = SiC + 2CO \quad (1)$$

However, the C/Si ratios in which single-phase SiC could be obtained were $1.0 < C/Si < 2.5$. This reason can be explained by some loss of volatilized SiO gas. The overall reaction in Eq. (1) can be divided into two stepwise elementary reactions:

$$SiO_2 + C = SiO + CO \quad (2)$$

$$SiO + 2C = SiC + CO \quad (3)$$

A part of the SiO gas volatilized by reaction (2) escapes from the system without the further reaction (3). In consequence, excess SiO_2 (i.e., lower C/Si ratio) is necessary to form SiC.

C. Vix-Guterl *et al.* showed that a β-SiC artefact is obtained by heat treatment of the carbon-silica artefact above 1743 K [27] and K. Janghorban and H. R. Tazesh prepared β-SiC by the pyrolysis of rice husks at 1623 K [28]. It is generally considered that SiC is formed by the

reaction of gaseous silicon monoxide (SiO) and carbon monoxide (CO) or carbon (C) in the carbothermal reduction. However, the reaction of SiO and CO becomes thermodynamically favorable when the partial pressure of CO is greater than 0.027 Mpa and the temperature is higher than 1573 K [21]. Also, R.V. Krishnarao and Y. R. Mahajan showed that the formation of considerable quantities of β-SiC whiskers was observed at 1573 K by pyrolysing raw rice husks in argon atmosphere [29]. In addition, J. Parmentier *et al.* suggested that high interface between carbon and silica leads to an almost complete conversion into SiC at temperature as low as 1523 K [30].

In the presence of pores (as explained in sections 3.2.1 and 3.2.2) in the composite bodies, carbothermal reactions could occur producing SiO and CO species; and when these gaseous species were entrapped in the porous structure, with P_{SiO}/P_{CO} ratio higher than one, SiC whisker particles could be produced at 1273 K. The reactions involved in this step can be summarized as [31]:

$$SiO_{(V)} + 3CO = SiC_{w(S)} + 2CO_{2(V)} \quad (4)$$

$$2C_{(S)} + 2CO_{2(V)} = 4CO_{(V)} \quad (5)$$

Hence, the overall reaction is:

$$SiO_{(V)} + 2C_{(S)} = SiC_{w(S)} + CO_{(V)} \quad (6)$$

Therefore, considering the above discussion and from the results of XPS and XRD analyses, we suggest that the formation of SiC by the carbothermic reduction of SiO_2 may be difficult at 1123K. On the other hand, the probability of formation of SiC is due the carbothermal reactions producing SiO and CO species; and when these gaseous species were entrapped in the porous structure could react to produce SiC particles, as given by Eq. (6).

3.5 Three point bend testing

Fig. 14 shows typical load-deflection curves obtained from the three-point-bend testing of dry and wet mixed pyrolyzed specimens. The load increases linearly with deflection and at the maximum load specimens broke in a brittle manner.

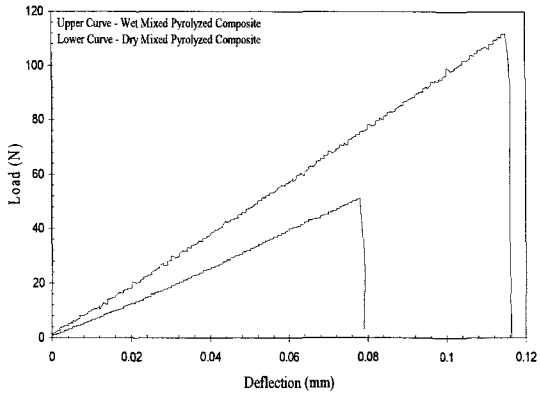

Fig. 14. Load-Deflection curves obtained for dry and wet mixed pyrolyzed specimens

According to the theory of bending of beams, the maximum bending stress (σ_{max}), which appears at the loading point, is used for evaluating the fracture strength of the composites. The maximum fracture stress that dry mixed pyrolyzed composite sustained was 13.9 MPa. Such low fracture strengths may be attributed to large pores existing in the specimens. On the other hand, wet mixed pyrolyzed specimen showed a maximum fracture stress of 56.04 MPa. This larger value of fracture stress of wet mixed pyrolyzed composite is due to the decrease in pore size and their filling by particles, as explained in section 3.2.2.

4. CONCLUSIONS

Preforms for porous ceramic-matrix-composite with well-defined pore architecture were fabricated with the pore size ranging from 844 nm to 8.44 μm by the pyrolysis of wet mixed powders. The decrease in pore size and their filling with particles resulted in a larger average apparent density (1.85 g/cm^3) than that of dry mixed pyrolyzed specimen (1.08 g/cm^3). EDS analyses showed that the matrices of both dry and wet mixed composites were composed of carbon; and small particles were nucleated due the agglomeration of nano sized zirconia particles that grown to large particles in the dry mixed pyrolyzed composite. On the other hand, the formation of small and large particles was not observed in wet mixing process, which means that zirconia particles are uniformly distributed in the composite. XPS analyses of the pyrolyzed specimens showed the formation of SiO_2, SiO and C that could react to produce β-SiC. In addition, XRD and XPS analyses of the pyrolyzed preforms strongly suggested the existence of β-SiC. The maximum fracture strength of the wet mixed pyrolyzed specimen was at most 56.04 MPa. Our experimental results have shown that this technique might be developed into a general pathway to prepare various porous composites with well-controlled pore structure.

REFERENCES

1. K. Maca, P. Dobsak and A.R. Boccaccini, *Ceramics International.*, 27 (2001) 577-584.
2. Toshihiro Isobe, Takahiro Tomita, Yoshikazu Kameshima, Akira Nakajima and Kiyoshi Okada, *Journal of the European Ceramic Society.*, 26 (2006) 957-960.
3. Mamoru Mizutani, Haruyuki Takase, Nobuyasu Adachi, Toshitaka Ota, Keiji Daimon and Yasuo Hikichi, *Science and Technology of Advance Materials.*, 6 (2005) 76-83.
4. Jian-Feng Yang, Shao-Yun Shan, Rolf Janssen, Gerold Schneider, Tatsuki Ohji, Shuzo Kanzaki, *Acta Materialia.*, 53 (2005) 2981-2990.
5. Yoshio Sakka, Fengiu Tang, Hiroshi Fudouzi and Tetsuo Uchikoshi, *Science and Technology of Advance Materials.*, 6 (2005) 915-920.
6. Sumin Zhu, Shuqiang Ding, Hong'an Xi, Qin Li and Ruoding Wang, *Ceramics International.*, Article in Press (2005) Ceri-2228 ; No. of Pages 4.
7. Fa-Zhi Zhang, Takeaki Kato, Masayoshi Fuji and Minoru Takahashi, *Journal of the European Ceramic Society.*, 26 (2006) 667-671.

8. Carmen Galassi, *Journal of the European Ceramic Society.*, Article in Press (2006) JECS-5953 ; No. of Pages 8.
9. V. D. Krstic, *Theoretical and Applied Fracture Mechanics.*, 45 (2006) 212-226.
10. W. D. Kingery, H. K. Bowen, and D. R. Uhlmann, "Introduction to Ceramics", Second Edition, John Wiley, John Wiley and sons Inc., New York, 1960, pp.791.
11. K. K. Chawla, "Ceramic Matrix Composites", First Edition, Chapman & Hall, London, 1993, pp.39, 45.
12. G. Ziegler, I. Richter and D. Suttor, *Composites.*, 30 (1999) 411-417.
13. Satya B. Sastri, James P. Armistead and Teddy M. Keller, *Carbon.*, 31 (4), (1993) 617-622.
14. Z. Laus evi and S. Marinkovi, Mechanical properties and chemistry of carbinization of phenol formaladehyde resin, Carbon 24 (5), (1986) 575-580.
15. Ramond A. Cutler and Kevin M. Rigtrup, *Journal of American Ceramic Society.*, 75 (1), (1992) 36-43.
16. J. I. Pena, H. Miao, R. I. Merino, G. F. de la Fuente and V. M. Orera, *Solid State Ionics.*, 101-103 (1997) 143-147.
17. Jagadish C. Ray, Ranjan K. Pati and P. Pramanik, *Journal of European Ceramic Society* 20 (2000) 1289-1295.
18. Chen-Chi M. Ma, Jia-Min Lin, Wen-Chi Chang and Tse-Hao Ko, *Carbon.*, 40 (2002) 977-984.
19. Paolo Bettotti, Gobind Das, Gino Mariotto, and Lorenzo Pavesi, *Applied Physics Letters.*, Volume 83, No. 4 (2003).
20. Zhicheng Liu, Weihua Shen, Wenbo Bu, Hangrong Chen, Zile Hua, Lingxia Zhang, Le Li, Jianlin Shi and Shouhong Tan, *Microporous and Mesoporous Materials.*, 82 (2005) 137-145.
21. Guo-Qiang Jin and Xiang-Yun Guo, *Microporous and Mesoporous Materials.*, 60 (2003) 207-212.
22. Soo-Jin Park and Yu-Sin Jang, *Journal of Colloid and Interface Science.*, 263 (2003) 170-176
23. C. D. Wagner, A. V. Naumkin, A. Kraut-Vass, J. W. Allison, C. J. Powell, and John R. Rumble Jr., "NIST X-ray Photoelectron Spectroscopy Database", (NIST Standard Reference Database 20, Version 3.4 (Web Version), *http://srdata.nist.gov/xps/index.htm).*
24. S.R. Dhakate and O.P. Bahl, *Carbon* 41 (2003) 1193-1203.
25. M. J. Guittet, J. P. Crocombette, and M. Gautier-Soyer, *Physical Review.*, B 63 (2001) 125117-125124.
26. Satoru Ishihara, Hidehiko Tanaka and Toshiyuki Nishimura, *Materials Research Society.*, 21(2006) 1167-1174.
27. C. Vix-Guterl, B. McEnaney and P. Ehrburger, *Journal of European Ceramic Society.*, 19 (1999) 427-432.
28. K. Janghorban and H. R. Tazesh, *Ceramic International* 25 (1999) 7-12.
29. R. V. Krishnarao and Y. R. Mahajan, *Ceramic International.*, 22 (1996) 353-358.
30. J. Parmentier, J. Patarin, J. Dentzer and C. Vix-Guterl, *Ceramic International.*, 28 (2002) 1-7.
31. Marco Antonio Schiavon, Eduardo Radovanic and Inez Valeria Pagotto Yoshida, *Powder Technology.*, 123 (2002) 232-241.

(Received August 1, 2006;Accepted August 10, 2007)